PERGAMON

International Journal of Solids and Structures 37 (2000) 7717–7730

INTERNATIONAL JOURNAL OF SOLIDS and STRUCTURES

www.elsevier.com/locate/ijsolstr

A semi-infinite interface crack interacting with subinterface matrix cracks in dissimilar anisotropic materials. I. Fundamental formulations and the *J*-integral analysis

Wen-Ye Tian, Yi-Heng Chen *

School of Civil Engineering and Mechanics, Xi'an Jiaotong University, Xi'an, Shaanxi Province 710049, People's Republic of China

Received 30 September 1998; in revised form 22 February 2000

Abstract

The *J*-integral analysis is presented for the interaction problem between a semi-infinite interface crack and subinterface matrix microcracks in dissimilar anisotropic materials. After deriving the fundamental solutions for an interface crack subjected to different loads and the fundamental solutions for an edge dislocation beneath the interface, the interaction problem is deduced to a system of singular integral equations with the aid of a superimposing technique. The integral equations are then solved numerically and a conservation law among three values of the *J*-integral is presented, which are induced from the interface crack tip, the microcracks and the remote field, respectively. The conservation law not only provides a necessary condition to confirm the numerical results derived, but also reveals that the microcrack shielding effect in such materials could be considered as a redistribution of the remote *J*-integral. It is this redistribution that does lead to the phenomenological shielding effect.

Keywords: Semi-infinite interface crack; Subinterface matrix microcrack; Dissimilar anisotropic materials

1. Introduction

Due to the potentialities of reducing weight and the capacities of optimizing the structural strength and stiffness, laminated fiber-reinforced composite materials are widely used in light structures and applied to replace many metallic components usually used before. However, the mechanical behaviors of such materials influenced by the fiber and matrix interaction, the matrix microcracks and the multi-ply configuration show very complicated features, which have challenged designers with a new class of problems. One particular area, which has received considerable attention in the past decade, has been their low tolerance to interfacial damage, and the other is concerned with the microdefects such as microcracks, microvoids, and microinclusions. The occurrence of these types of damage, which are frequently caused by impact or other

* Corresponding author. Tel.: +86-29-266-0404; fax: +86-29-323-7910.
E-mail address: yhchen2@xjtu.edu.cn (Y.-H. Chen).

0020-7683/00/$ - see front matter
PII: S0020-7683(00)00117-7

sources, are common and unavoidable during manufacturing, maintenance, and service of the light structures.

To date, although many significant progresses have been made in solving the interface crack problems in both dissimilar isotropic materials and dissimilar anisotropic materials (Wang and Choi, 1983a,b; Hutchinson et al., 1987; Rice, 1988; Suo, 1990; Ting, 1986, 1990; Gao, 1991; Lu and Lardner, 1992; Chen and Hasebe, 1994a,b), the influence of microcracks in the process zone near the tip of an interface macrocrack in dissimilar anisotropic materials on the tip parameters remains inadequately treated.

On the other hand, recent investigations reveal that the well-known J-integral (Rice, 1968) plays an important role in treating the interaction problem between a macrocrack and near-tip microcracks in brittle materials or in bimaterial isotropic solids (Chen, 1996; Zhao and Chen, 1997). It is found that there exists an inherent relation among three values of the J-integral, respectively, induced from the macrocrack tip, the microcracks near the tip, and the remote stresses. It seems that the J-integral should play the similar role when the interaction problem in dissimilar anisotropic materials is considered.

The aim of this paper is to investigate the interaction behaviors between a semi-infinite interface crack and multiple subinterface matrix microcracks in the near tip process zone in dissimilar anisotropic materials. In Section 2, the fundamental solutions, respectively, for a semi-infinite interface crack subjected to different kinds of loads and for an edge dislocation beneath the interface in a dissimilar anisotropic materials are given. In Section 3, the pseudo-traction method is combined with the edge dislocation method (abbreviated as PTEDM) to solve the interaction problem. A superimposing technique is adopted to deduce the interaction problem mentioned above to a system of singular integral equations whose solutions could be given numerically. In order to confirm numerical results and to avoid mistakes in the manipulations, the J-integral analysis is performed in Section 4 by introducing three different closed contours specially defined. In Section 5, numerical results are given for a composite material whose anisotropic material constants are used by Sih and Chen (1981). The derived results reveal that a consistency check based on the J-integral analysis really exists, which not only confirms the numerical results themselves, but also shows the redistribution nature of the remote J-integral. Finally, major conclusions derived in Part I of this series are summarized.

2. Fundamental formulations in dissimilar anisotropic materials

Recently, the interface crack problem in anisotropic materials has been studied by Suo (1990). It is well known that under plane stress or plane strain conditions, the elastic field in an anisotropic material could be represented in terms of two complex functions $f_1(z_1)$ and $f_2(z_2)$, each of which is holomorphic in its argument $z_j = x + \mu_j y$, $(j = 1, 2)$. Here, μ_j denotes two distinct complex numbers with positive imaginary parts. They could be determined as the roots of a fourth-order characteristic equation (Lekhnitskii, 1963). Using these holomorphic functions, the representations of displacements u_i, stresses σ_{ji}, and resultant forces T_i could be put in the following forms:

$$u_i = 2\mathrm{Re}\left[\sum_{j=1}^{2} A_{ij} f_j(z_j)\right], \quad T_i = -2\mathrm{Re}\left[\sum_{j=1}^{2} L_{ij} f_j(z_j)\right], \quad \sigma_{2i} = 2\mathrm{Re}\left[\sum_{j=1}^{2} L_{ij} f_j'(z_j)\right],$$
$$\sigma_{1i} = -2\mathrm{Re}\left[\sum_{j=1}^{2} L_{ij}\mu_j f_j'(z_j)\right] \qquad (i = 1, 2), \tag{1}$$

where the over prime is designated as the derivative with respect to the associated arguments, and $\mathbf{L}$ and $\mathbf{A}$ are two 2×2 complex matrices depending on elastic constants (Suo, 1990)

$$\mathbf{L} = \begin{bmatrix} -\mu_1 & -\mu_2 \\ 1 & 1 \end{bmatrix}, \tag{2}$$

$$\begin{aligned} A_{1j} &= s_{11}\mu_j^2 + s_{12} - s_{16}\mu_j \\ A_{2j} &= s_{21}\mu_j + s_{22}/\mu_j - s_{26} \end{aligned} \quad (j = 1, 2), \tag{3}$$

where, μ_j satisfies the following fourth-order characteristic equation:

$$s_{11}\mu^4 - 2s_{16}\mu^3 + (2s_{12} + s_{66})\mu^2 - 2s_{26}\mu + s_{22} = 0. \tag{4}$$

Eqs. (2)–(4) are valid for plane stress deformation, while the corresponding ones for plane strain deformation could be given by using the following change of compliances

$$\tilde{s}_{ij} = s_{ij} - s_{i3}s_{j3}/s_{33}. \tag{5}$$

Suo (1990) has introduced a positive definite Hermitian matrix **B**

$$\mathbf{B} = \mathrm{i}\mathbf{A}\mathbf{L}^{-1}, \tag{6}$$

where $\mathrm{i} = \sqrt{-1}$. For interface problems in dissimilar anisotropic materials in which materials 1 and 2 occupy the upper and lower half planes, respectively (Fig. 1), another positive-definite Hermitian matrix **H** involving bimaterial elastic constants is defined as follows (Suo, 1990):

$$\mathbf{H} = \mathbf{B}_1 + \overline{\mathbf{B}}_2, \tag{7}$$

where subscripts 1 and 2 are attached to the upper and lower materials, respectively, the over bar denotes the corresponding complex conjugate.

Furthermore, Suo (1990) has also defined the following function vector $\mathbf{f}(z)$:

$$\mathbf{f}(z) = [f_1(z), f_2(z)]^{\mathrm{T}}, \tag{8}$$

where $f_1(z)$ and $f_2(z)$ describe the functions for the upper and lower materials, respectively.

Once the solution of $\mathbf{f}(z)$ is derived for a given boundary value problem, a replacement of z_1 or z_2 should be made for each component function to calculate field quantities from Eq. (1). Moreover, the set of vectors along the interface is given as follows:

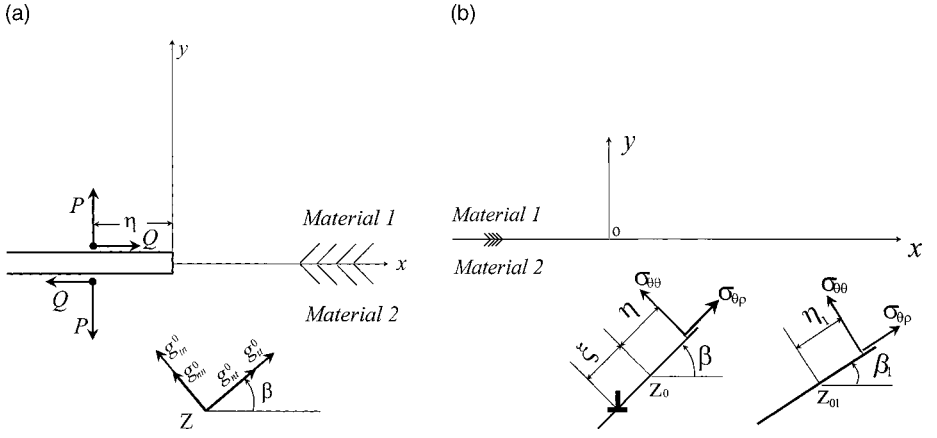

Fig. 1. (a) A pair of normal and tangential concentrated tractions acting on an interface macrocrack. (b) An edge dislocation near the interface.

$$\begin{aligned}\mathbf{u}_x &= \{u_j(x,0)\} = \mathbf{A}\mathbf{f}(x) + \overline{\mathbf{A}}\bar{\mathbf{f}}(x),\\ \mathbf{t}(x) &= \{\sigma_{2j}(x,0)\} = \mathbf{L}\mathbf{f}'(x) + \overline{\mathbf{L}}\bar{\mathbf{f}}'(x),\end{aligned} \tag{9}$$

where the x-axis is along the interface.

2.1. Fundamental solution for an interface crack

The formulations presented above are used to derive the fundamental solution for a semi-infinite interface crack under concentrated tractions as shown in Fig. 1(a). Without going into detail (Appendix A), the following Hilbert problem is deduced:

$$\mathbf{h}^+(x) + \overline{\mathbf{H}}^{-1}\mathbf{H}\mathbf{h}^-(x) = \mathbf{t}_0(x), \quad x \in C, \tag{10}$$

where C is the crack surface, the complete solution could easily be given as follows:

$$\mathbf{h}(z) = h_1(z)\mathbf{w} + h_2(z)\overline{\mathbf{w}}, \tag{11}$$

where

$$h_1(z) = \frac{\chi(z)}{2\pi \mathrm{i}} \int_c \frac{t_{01}(x)\,\mathrm{d}x}{\chi^+(x)(x-z)}, \tag{12}$$

$$h_2(z) = \frac{\overline{\chi}(z)}{2\pi \mathrm{i}} \int_c \frac{\bar{t}_{01}(x)\,\mathrm{d}x}{\overline{\chi}^+(x)(x-z)}, \tag{13}$$

$$t_{01} = \frac{\overline{\mathbf{w}}\mathbf{H}\mathbf{t}_0(x)}{\overline{\mathbf{w}}\mathbf{H}\mathbf{w}}, \tag{14}$$

$$\chi(z) = z^{-1/2-\mathrm{i}\varepsilon}, \tag{15}$$

and the vector $\mathbf{w}$ and the index ε satisfy the following equation:

$$\overline{\mathbf{H}}\mathbf{w} = \mathrm{e}^{2\pi\varepsilon}\mathbf{H}\mathbf{w}. \tag{16}$$

It should be pointed out that for the case in Fig. 1(a),

$$\mathbf{t}_0(x) = [0, P\delta(x-\eta)]^{\mathrm{T}} \quad \text{for the traction } P, \tag{17a}$$

$$\mathbf{t}_0(x) = [Q\delta(x-\eta), 0]^{\mathrm{T}} \quad \text{for the traction } Q, \tag{17b}$$

where η is the distance of the traction point from the origin (Fig. 1(a)).

Therefore, the stresses at any point z below the interface (Fig. 1(a)) induced from the tractions P and Q, respectively, could be evaluated by using Eqs. (11), (A.7), and (1), without any difficulty. As well-known (Zhao and Chen, 1997; Chen 1996), the stresses could be considered as the influence functions or the kernel functions in the boundary element method, which will be denoted below by g^0_{nn} and g^0_{nt} for the traction P and g^0_{tn} and g^0_{tt} for the traction Q, respectively.

2.2. Fundamental solution for an edge dislocation

An edge dislocation below the interface is shown in Fig. 1(b). The potentials f_k modeling a dislocation singularity near a bimaterial interface in an anisotropic body are proposed by Miller (1989)

$$f_k'(z) = \frac{B_k}{z - z_{0k}} - \sum_{j=1}^{4} b_{kj} \sum_{i=1}^{2} \overline{m_{ji}} \frac{\overline{B_i}}{z - \overline{z_{0i}}} \tag{18}$$

in which $z_{0k} = x_0 + \mu_k y_0$ represents a specified point $z_0(x_0, y_0)$ locating the singularity, and

$$\begin{bmatrix} b_{1j} \\ b_{2j} \\ b_{3j} \\ b_{4j} \end{bmatrix} = \begin{bmatrix} \begin{pmatrix} A_{11} & A_{12} \\ A_{21} & A_{22} \end{pmatrix}_2 & \begin{pmatrix} -\overline{A_{11}} & -\overline{A_{12}} \\ -\overline{A_{21}} & -\overline{A_{22}} \end{pmatrix}_1 \\ \begin{pmatrix} L_{21} & L_{22} \\ L_{11} & L_{12} \end{pmatrix}_2 & \begin{pmatrix} -\overline{L_{21}} & -\overline{L_{22}} \\ -\overline{L_{11}} & -\overline{L_{12}} \end{pmatrix}_1 \end{bmatrix}^{-1} \tag{19}$$

$$m_{1k} = (A_{1k})_2, \quad m_{2k} = (A_{2k})_2, \quad m_{3k} = (L_{2k})_2, \quad m_{4k} = (L_{1k})_2, \tag{20}$$

where the formations $(\cdot)_1$ and $(\cdot)_2$ correspond to the upper and the lower materials, respectively.

In addition, $B_k (k = 1, 2)$ satisfies the following equation (Miller, 1989):

$$\begin{aligned} &\mathrm{Im}(B_1 + B_2) = 0, \\ &\mathrm{Im}(\mu_1 B_1 + \mu_2 B_2) = 0, \\ &\mathrm{Im}(A_{11} B_1 + A_{12} B_2) = -\frac{B_x}{4\pi}, \\ &\mathrm{Im}(A_{21} B_1 + A_{22} B_2) = -\frac{B_y}{4\pi}, \end{aligned} \tag{21}$$

where B_x and B_y are the displacement discontinuities across the dislocation line in the x and y directions, respectively.

From Eqs. (1) and (18), the stresses field due to the edge dislocation at any point $z = z_0 + \xi e^{i\beta}$ near the interface are formulated in a polar coordinate system (Fig. 1(b)),

$$\sigma_{\theta\theta} + i\sigma_{\rho\theta} = \Lambda_1(\xi, \eta, \beta) + \Lambda_3(\xi, \eta, \beta, y_0) + \Lambda_2(\xi, \eta, \beta) + \Lambda_4(\xi, \eta, \beta, y_0), \tag{22}$$

for any point $z = z_0 + \eta e^{i\beta}$, and

$$\begin{aligned} \sigma_{\theta\theta} + i\sigma_{\rho\theta} = {} & \Lambda_5(\xi, \beta, x_0, y_0, \eta_1, \beta_1, x_{01}, y_{01}) + \Lambda_7(\xi, \beta, x_0, y_0, \eta_1, \beta_1, x_{01}, y_{01}) \\ & + \Lambda_6(\xi, \beta, x_0, y_0, \eta_1, \beta_1, x_{01}, y_{01}) + \Lambda_8(\xi, \beta, x_0, y_0, \eta_1, \beta_1, x_{01}, y_{01}), \end{aligned} \tag{23}$$

for any point $z = z_{01} + \eta_1 e^{i\beta_1}$. Moreover, it should be emphasized that $\beta_1 = 0$, $x_{01} = 0$, and $y_{01} = 0$, when point z falls into the interface, where the eight functions ($\Lambda_1 \sim \Lambda_8$) are given in Appendix B. The influence functions or the kernel functions used below could be evaluated by Eqs. (22) and (23).

2.3. Remote loading conditions

Consider a semi-infinite interface crack in an infinite dissimilar anisotropic material loaded by the remote stress intensity factors K_1^∞ and K_2^∞, the potentials for the two half spaces are

$$\mathbf{L}_1 \mathbf{f}_1'(z) = \frac{e^{\pi\varepsilon} K z^{i\varepsilon} w + e^{-\pi\varepsilon} \overline{K} z^{-i\varepsilon} \overline{w}}{2(2\pi z)^{\frac{1}{2}} \cosh \pi\varepsilon} \quad (z \in \text{material 1}), \tag{24a}$$

$$\mathbf{L}_2 \mathbf{f}_2'(z) = \frac{e^{-\pi\varepsilon} K z^{i\varepsilon} w + e^{\pi\varepsilon} \overline{K} z^{-i\varepsilon} \overline{w}}{2(2\pi z)^{\frac{1}{2}} \cosh \pi\varepsilon} \quad (z \in \text{material 2}), \tag{24b}$$

where $K = K_1^\infty + iK_2^\infty$.

When calculating the field quantities via Eq. (1), it is necessary to replace z by $z_j = x + \mu_j y$, respectively, for each component of $f(z)$ in Eq. (24a) or Eq. (24b) as treated by Suo (1990).

Consequently, the residual stresses to be released on the location of subinterface crack are given as

$$\begin{aligned} p &= 2\mathrm{Re}[f_1'(z_1) + f_2'(z_2)], \\ q &= -2\mathrm{Re}[\mu_1 f_1'(z_1) + \mu_2 f_2'(z_2)], \end{aligned} \tag{25}$$

where $f_1'(z_1)$ and $f_2'(z_2)$ are given by Eq. (24a) or Eq. (24b).

3. Superimposing technique and singular integral equations

Consider N subinterface microcracks near the tip of a semi-infinite interface macrocrack (Fig. 2(a)). Here, the prescribed stress intensity factors K_1^∞ and K_2^∞ are taken to specify the applied remote stress field. Using the pseudo-traction method proposed by Horii and Nemat-Nasser (1985), the problem shown in Fig. 2(a) is decomposed into $N+2$ subproblem (Fig. 2(b)–(d)), each of which contains one single crack. The unknown normal tractions $P_0(t), P_l(s_l)$and shear tractions $Q_0(t), Q_l(s_l)$ on the crack faces are the so-called pseudo-tractions to be determined. Furthermore, each subinterface crack with length $2a_l\ (l = 1, 2, \ldots, N)$ could be modeled by edge dislocation distributed continuously at the crack location. Using the superimposing technique, the following integral equations are reduced as Zhao and Chen (1997) did, in which $P_l(x_l)$ and $Q_l(x_l)$ are expressed in the form of continuously distributed dislocations (Lu and Lardner, 1992).

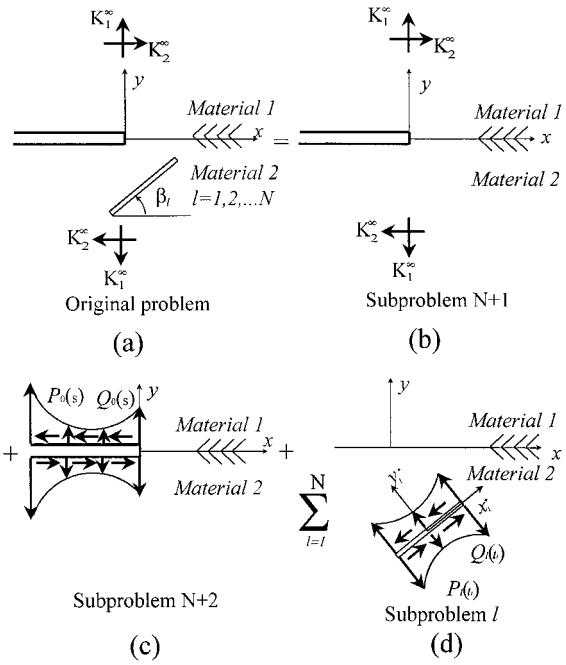

Fig. 2. Method of superimposing.

$$P_0(\eta)+\mathrm{Re}\sum_{l=1}^{N}\int_{-a_l}^{a_l}[\Lambda_5(\xi_l,\beta_l,x_{0l},y_{0l},\eta,0,0,0)+\Lambda_7(\xi_l,\beta_l,x_{0l},y_{0l},\eta,0,0,0)+\Lambda_6(\xi_l,\beta_l,x_{0l},y_{0l},\eta,0,0,0)+\Lambda_8(\xi_l,\beta_l,x_{0l},y_{0l},\eta,0,0,0)]\,\mathrm{d}\xi_l=0, \tag{26a}$$

$$Q_0(\eta)+\mathrm{Im}\sum_{l=1}^{N}\int_{-a_l}^{a_l}[\Lambda_5(\xi_l,\beta_l,x_{0l},y_{0l},\eta,0,0,0)+\Lambda_7(\xi_l,\beta_l,x_{0l},y_{0l},\eta,0,0,0)+\Lambda_6(\xi_l,\beta_l,x_{0l},y_{0l},\eta,0,0,0)+\Lambda_8(\xi_l,\beta_l,x_{0l},y_{0l},\eta,0,0,0)]\,\mathrm{d}\xi_l=0, \tag{26b}$$

$$\int_{-\infty}^{0}P_0(\eta)g^0_{nn,0l}(\eta,\eta_l)\,\mathrm{d}\eta+\int_{-\infty}^{0}Q_0(\eta)g^0_{tn,0l}(\eta,\eta_l)\,\mathrm{d}\eta+\mathrm{Re}\left\{\int_{-a_l}^{a_l}[\Lambda_1(\xi_l,\eta_l,\beta_l)+\Lambda_3(\xi_l,\eta_l,\beta_l,y_{0l})+\Lambda_2(\xi_l,\eta_l,\beta_l)+\Lambda_4(\xi_l,\eta_l,\beta_l,y_{0l})]\,\mathrm{d}\xi_l+\sum_{\substack{i=1\\ i\neq l}}^{N}\int_{-a_i}^{a_i}[\Lambda_5(\xi_i,\beta_i,x_{0i},y_{0i},\eta_l,\beta_l,x_{0l},y_{0l})+\Lambda_7(\xi_i,\beta_i,x_{0i},y_{0i},\eta_l,\beta_l,x_{0l},y_{0l})+\Lambda_6(\xi_i,\beta_i,x_{0i},y_{0i},\eta_l,\beta_l,x_{0l},y_{0l})+\Lambda_8(\xi_i,\beta_i,x_{0i},y_{0i},\eta_l,\beta_l,x_{0l},y_{0l})]\,\mathrm{d}\xi_i\right\}=p_l(\eta_l) \tag{26c}$$

$$\int_{-\infty}^{0}P_0(\eta)g^0_{nt,0l}(\eta,\eta_l)\,\mathrm{d}\eta+\int_{-\infty}^{0}Q_0(\eta)g^0_{tt,0l}(\eta,\eta_l)\,\mathrm{d}\eta+\mathrm{Im}\left\{\int_{-a_l}^{a_l}[\Lambda_1(\xi_l,\eta_l,\beta_l)+\Lambda_3(\xi_l,\eta_l,\beta_l,y_{0l})+\Lambda_2(\xi_l,\eta_l,\beta_l)+\Lambda_4(\xi_l,\eta_l,\beta_l,y_{0l})]\,\mathrm{d}\xi_l+\sum_{\substack{i=1\\ i\neq l}}^{N}\int_{-a_i}^{a_i}[\Lambda_5(\xi_i,\beta_i,x_{0i},y_{0i},\eta_l,\beta_l,x_{0l},y_{0l})+\Lambda_7(\xi_i,\beta_i,x_{0i},y_{0i},\eta_l,\beta_l,x_{0l},y_{0l})+\Lambda_6(\xi_i,\beta_i,x_{0i},y_{0i},\eta_l,\beta_l,x_{0l},y_{0l})+\Lambda_8(\xi_i,\beta_i,x_{0i},y_{0i},\eta_l,\beta_l,x_{0l},y_{0l})]\,\mathrm{d}\xi_i\right\}=q_l(\eta_l). \tag{26d}$$

In addition, the uniform conditions require that

$$\int_{-a_l}^{a_l}B_x(\xi_l)\,\mathrm{d}\xi_l=0,\quad \int_{-a_l}^{a_l}B_y(\xi_l)\,\mathrm{d}\xi_l=0, \tag{27}$$

and $\Lambda_1,\Lambda_2,\Lambda_3,\Lambda_4,\Lambda_5,\Lambda_6,\Lambda_7$, and Λ_8 are given in Appendix B, $-a_l<\xi_l<a_l,-a_l<\eta_l<a_l(l=1,2,\ldots,N)$, $-\infty<\eta<0$, $B_x(\xi)$ and $B_y(\xi)$ are dislocation density functions; $p_l(\eta_l)$ and $q_l(\eta_l)$ are given by Eq. (25).

The integral equation (26) could be solved numerically by using the Chebyshev numerical integration and the Chebyshev polynomial technique, if $B(\xi)$ is expressed by the first kind of Chebyshev polynomial as follows:

$$B_x(\xi_l)=\frac{1}{\sqrt{1-\gamma_l^2}}\sum_{k=0}^{M}d_kT_k(\gamma_l), \tag{28}$$

$$B_y(\xi_l) = \frac{1}{\sqrt{1-\gamma_l^2}} \sum_{k=0}^{M} b_k T_k(\gamma_l), \tag{29}$$

where $-1 < \gamma_l = \xi_l/a_l < 1, -a_l \leqslant \xi_l \leqslant a_l$, d_k, b_k are coefficients of the Chebyshev polynomial to be determined, M indicates the number of the Gauss–Chebyshev collocation points.

Once the Eqs. (26a)–(26d) is solved, the incremental values of the stress intensity factors (SIFs) at the macrocrack tip and SIFs at both tips of the microcrack could be evaluated.

The stress intensity factor for the semi-infinite interface crack under arbitrarily distributed loads $P_0(x)$ and $Q_0(x)$ defined by Suo (1990) is

$$K = K_1 + \mathrm{i}K_2 = -\left(\frac{2}{\pi}\right)^{1/2} \cosh \pi\varepsilon \int_{-\infty}^{0} (-x)^{-\frac{1}{2}-\mathrm{i}\varepsilon} t_{01}(x)\,\mathrm{d}x, \tag{30}$$

$$t_{01}(x) = \frac{\overline{\mathbf{w}}^{\mathrm{T}}\mathbf{H}[Q_0(x), P_0(x)]}{\overline{\mathbf{w}}^{\mathrm{T}}\mathbf{H}\mathbf{w}}.$$

$\mathbf{w}$ and $\mathbf{H}$ are given in Eq. (16). With the solutions of $P_0(x)$ and $Q_0(x)$ in Eq. (26), K could be calculated by using the Chebyshev numerical integration method.

For the finite subinterface crack l, the stress intensity factor at the right tip ($\xi = a_l$) described by $B(\xi)$ is

$$K = K_1 + \mathrm{i}K_2 = \frac{(2\pi)^{3/2}}{\sqrt{a_l}} \left\{ \sum_{k=1}^{2} \frac{\left[1 + \mu_k^2 + \mathrm{e}^{2\mathrm{i}\beta}(1 - \mu_k^2 - 2\mathrm{i}\mu_k)\right] B_k(a_l)}{(1 - \mathrm{i}\mu_k)\mathrm{e}^{\mathrm{i}\beta} + (1 + \mathrm{i}\mu_k)\mathrm{e}^{-\mathrm{i}\beta}} + \frac{\left[1 + \overline{\mu_k}^2 + \mathrm{e}^{2\mathrm{i}\beta}(1 - \overline{\mu_k}^2 - 2\mathrm{i}\overline{\mu_k})\right] \overline{B_k}(a_l)}{(1 + \mathrm{i}\overline{\mu_k})\mathrm{e}^{-\mathrm{i}\beta} + (1 - \mathrm{i}\overline{\mu_k})\mathrm{e}^{\mathrm{i}\beta}} \right\} \tag{31}$$

with an analogous expression at the left tip. With the solutions of Eqs. (26), (B.1), (21), (28) and (29), K could be evaluated numerically.

4. Analysis of the *J*-integral

It is well known that the J-integral (Rice, 1968) has a definite physical significance as the total potential energy release rate, which is defined as

$$J = \int_{\Gamma} [w(\varepsilon) n_1 - \sigma_{ij} n_j u_{i,1}]\,\mathrm{d}s, \tag{32}$$

where n_j signifies the outer normal of the contour Γ which is a closed contour to be chosen. Customarily, for single crack problem, Γ is generally taken as a smooth curve that starts from one point on the lower face and ends at another point on the upper face of a crack.

Considering the original problem with three integral contours as shown in Fig. 3, it is easy to get the following consistent relation among three values of the J-integral, respectively, calculated along the three integral contours in Fig. 3 (Chen, 1996):

$$\frac{J_t}{J_\infty} + \frac{\Delta J}{J_\infty} = 1, \tag{33}$$

where J_∞ and J_t are given in Appendix C, and

$$\Delta J = J_1^* \cos\beta - J_2^* \sin\beta, \tag{34}$$

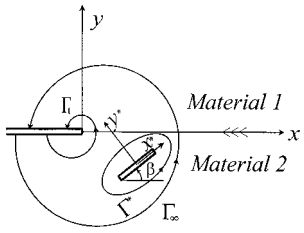

Fig. 3. An interface macrocrack and a subinterface microcrack with three integral contours.

where β is the angle measured from x-axis to x^*-axis (Fig. 3), the star denotes the local coordination system, and J_1^* and J_2^* are given in Appendix C.

In the above equations, J_∞, J_t and J_1^* can also be expressed in the following forms (Suo, 1990):

$$\begin{aligned} J_\infty &= \overline{\mathbf{w}}^{\mathrm{T}}(\mathbf{H}+\overline{\mathbf{H}})\mathbf{w}\left|K_1^\infty + \mathrm{i}K_2^\infty\right|^2/(4\cosh^2\pi\varepsilon),\\ J_t &= \overline{\mathbf{w}}^{\mathrm{T}}(\mathbf{H}+\overline{\mathbf{H}})\mathbf{w}\left|K_1^\infty + \Delta K_1 + \mathrm{i}(K_2^\infty + \Delta K_2)\right|^2/(4\cosh^2\pi\varepsilon),\\ J_1^* &= \tfrac{1}{4}(\mathbf{K}^{\mathrm{R}})^{\mathrm{T}}\mathbf{Y}^*\mathbf{K}^{\mathrm{R}} - \tfrac{1}{4}(\mathbf{K}^{\mathrm{L}})^{\mathrm{T}}\mathbf{Y}^*\mathbf{K}^{\mathrm{L}}, \end{aligned} \tag{35}$$

where $\mathbf{Y}^* = 2\mathrm{Re}(\mathrm{i}\mathbf{A}^*\mathbf{L}^{*-1})$, $\mathbf{L}^*$ and $\mathbf{A}^*$ are given in Eqs. (2) and (3), $\mathbf{K}^{\mathrm{R}} = [K_2^{\mathrm{R}}, K_1^{\mathrm{R}}]^{\mathrm{T}}$, and $\mathbf{K}^{\mathrm{L}} = [K_2^{\mathrm{L}}, K_1^{\mathrm{L}}]^{\mathrm{T}}$ whose elements K_1 and K_2 are stress intensity factors, the superscripts R and L refer to the right and left tip of the microcrack, respectively.

However, the calculation of J_2^* should specially be considered since it consists of two parts, one of which is induced from both microcracks tips and the other from the microcrack traction free faces (Herrmann and Herrmann, 1981).

The contribution of the right crack tip to the J_2^*-integral, namely $J_2^{t\mathrm{R}}$, should be equal to the energy release rate specially proposed by Chen and Ma (1997):

$$J_2^{t\mathrm{R}} = \lim_{\Delta\to 0}\frac{-1}{2\Delta}\int_0^\Delta \sigma_{i1}^*(\Delta - r)u_i^*(r)\,\mathrm{d}r, \tag{36}$$

where $\sigma_{i1}(r)$ and $u_i(r)$ is the stress at a distance r ahead the right crack tip and the displacement jump at a distance r behind the right crack tip, respectively:

$$\begin{aligned} \sigma_{i1}^*(r) &= \mathbf{X}^*\mathbf{K}^{\mathrm{R}}(2\pi r)^{-1/2},\\ u_i^*(r) &= \mathbf{Y}^*\mathbf{K}^{\mathrm{R}}(2r/\pi)^{1/2}, \end{aligned} \tag{37}$$

where the superscript R refers to the right tip of the microcrack, and the matrices

$$\begin{aligned} \mathbf{X}^* &= -\mathrm{Re}(\mathbf{D}^*\mathbf{L}^{*-1}),\\ \mathbf{D}^* &= \begin{bmatrix} L_{11}^*\mu_1^* & L_{12}^*\mu_2^* \\ L_{21}^*\mu_1^* & L_{22}^*\mu_2^* \end{bmatrix}. \end{aligned} \tag{38}$$

Substituting Eq. (37) into Eq. (36), the contribution of the right crack tip to the J_2^*-integral is obtained explicitly as:

$$J_2^{t\mathrm{R}} = \tfrac{1}{4}(\mathbf{K}^{\mathrm{R}})^{\mathrm{T}}\mathbf{X}^*\mathbf{Y}^*\mathbf{K}^{\mathrm{R}}. \tag{39}$$

The contribution of the left tip to the J_2^*-integral, namely $J_2^{t\mathrm{L}}$, could be given in a similar way

$$J_2^{t\mathrm{L}} = -\tfrac{1}{4}(\mathbf{K}^{\mathrm{L}})^{\mathrm{T}}\mathbf{X}^*\mathbf{Y}^*\mathbf{K}^{\mathrm{L}}. \tag{40}$$

Following the conclusion derived by Herrmann and Herrmann (1981), the contribution of the crack faces to the J_2^*-integral could be derived as

$$J_2^f = \int_{-a}^{a} (\omega^+ - \omega^-)\,\mathrm{d}x, \tag{41}$$

where ω^+ and ω^- are the boundary values of the strain energy densities on the upper and lower crack faces, respectively.

Thus, the J_2^*-integral calculated along the contour surrounding the complete crack is

$$J_2^* = \frac{1}{4}(\mathbf{K}^{\mathrm{R}})^{\mathrm{T}}\mathbf{X}^*\mathbf{Y}^*\mathbf{K}^{\mathrm{R}} - \frac{1}{4}(\mathbf{K}^{\mathrm{L}})^{\mathrm{T}}\mathbf{X}^*\mathbf{Y}^*\mathbf{K}^{\mathrm{L}} + \int_{-a}^{a} (\omega^+ - \omega^-)\,\mathrm{d}x^*. \tag{42}$$

Using the superimposing technique, the above results can be extended to the multiple subinterface microcracks situation. Assuming that there exist N subinterface microcracks, the consistent relation (33) becomes

$$\frac{J_t}{J_\infty} + \sum_{1}^{N} \frac{\Delta J}{J_\infty} = 1. \tag{43}$$

Eq. (43) shows the inherent law of the J-integral whose values are induced from the subinterface microcracks ($\sum \Delta J/J_\infty$) and the tip of the interface macrocrack (J_t/J_∞), respectively. This has been proved to be valid in brittle solids and in bimaterial isotropic solids (Chen, 1996; Zhao and Chen, 1997). Moreover, it provides a necessary condition as well as a powerful tool to examine the numerical results derived by the technique PTEDM proposed in this part.

5. Numerical results and consistency check

In this section, the properties of the upper material are taken to be an anisotropic material, whose material constants are $E_1 = 5.50 \times 10^6$ psi, $E_2 = E_3 = 1.33 \times 10^6$ psi, $G_{21} = 0.50 \times 10^6$ psi, $v_{12} = 0.28$, $v_{23} = 0.36$ (Sih and Chen, 1981), while whose fiber direction is along the interface. On the contrary, the lower material is taken to be the same material but its fiber direction is perpendicular to the plane under consideration (the isotropic case, i.e., $E_1 = E_2 = 1.33 \times 10^6$ psi). Therefore, matrix microcracks could be formed near an interface crack tip in the lower material.

Assume a semi-infinite interface macrocrack interacted with a subinterface matrix microcrack of length $2a$ in the near-tip process zone as shown in Fig. 4. Here, r is the distance between the macrocrack tip and the center of the subinterface microcrack, α is the angle between r and the x-axis, and β is the angle of the subinterface microcrack with respect to the x-axis. The remote stress field is specified by the intensity K_{I}^{∞} only. Let $\beta = 30°$ and $45°$, respectively, and $r/a = 2.0$, the computed values of J_t/J_∞ and $\Delta J/J_\infty$ against the location angle α are shown in Fig. 5. From Fig. 5, it is found that the consistent relation of the J-integral is really satisfied, i.e., the computed values of J_t/J_∞ plus the computed values of $\Delta J/J_\infty$ always equal to unit. This confirms that the PTEDM proposed in this paper is effective for solving the interaction problem in dissimilar anisotropic materials, although the different mismatch nature from those by Zhao and Chen (1997) is taken into account. Moreover, the relation actually provides a powerful tool to check the numerical results no matter how they are derived.

It is also shown that the microcrack has the amplification effect on J_t for smaller values of the location angle ($\alpha < 60°$ for $\beta = 30°$, and $\alpha < 54°$ for $\beta = 45°$) corresponding to the normalized value $J_t/J_\infty > 1$, while the microcrack has the shielding effect on J_t for larger values of the location angle corresponding to

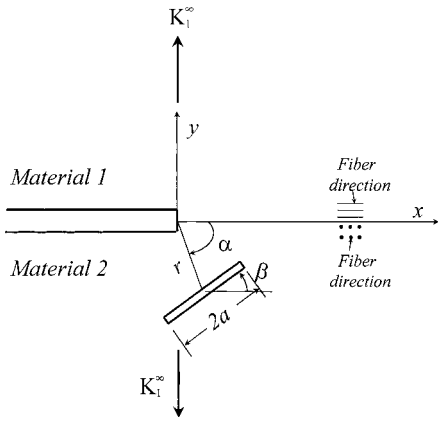

Fig. 4. An interface crack and a subinterface microcrack.

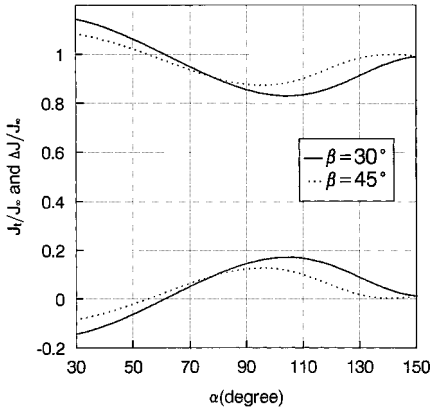

Fig. 5. J_t/J_∞ and $\Delta J/J_\infty$ vs. the angle α.

the value $J_t/J_\infty < 1$. Moreover, there is only single neutral shielding angle for each curve at which a transform from the amplification effect to the shielding effect occurs.

6. Conclusion

From the foregoing manipulations and discussions, it is concluded that,

(1) PTEDM is really effective to solve the interaction problem between a semi-infinite interface crack and multiple subinterface microcracks in dissimilar anisotropic materials.

(2) The simple but universal relation (43) found in brittle solids (Chen, 1996) and in bimaterial isotropic solids (Zhao and Chen, 1997) among three values of the J-integral induced from the interface macrocrack tip, the subinterface microcracks, and the remote stress field, respectively, is still valid in dissimilar anisotropic solids, although the material mismatch nature influences the near-tip stress field.

(3) The microcrack shielding effect in dissimilar anisotropic materials could be considered, from the physical point of view, as the redistribution of the J-integral. As pointed out by Hutchinson (1987), there

are two sources of the redistribution of stress in the near-tip stress field of a macrocrack induced from microcracks. One is due to the reduction in the effective elastic moduli and the other is the strain arising from the release of residual stresses. Obviously, it is this redistribution of stresses in the near-tip stress field that does lead to the redistribution of the J-integral.

In Part II of this series, numerical results of the interaction between a semi-infinite interface crack and multiple subinterface matrix microcracks will be shown in figures and tables and studied in detail. The major behaviors of the interaction against the multiple microcrack configurations are discussed.

Acknowledgements

This work was supported by the Chinese National Natural Science Foundation, and the Doctorate Foundation of Xi'an Jiaotong University.

Appendix A

According to the continuous condition of the traction across the whole x-axis (see Fig. 1(a)), there is

$$\mathbf{L}_1\mathbf{f}_1'(x) + \overline{\mathbf{L}}_1\bar{\mathbf{f}}_1'(x) = \mathbf{L}_2\mathbf{f}_2'(x) + \overline{\mathbf{L}}_2\bar{\mathbf{f}}_2'(x) \tag{A.1}$$

to facilitate the analytic continuation, Eq. (A.1) is rearranged as

$$\mathbf{L}_1\mathbf{f}_1'(x) - \overline{\mathbf{L}}_2\bar{\mathbf{f}}_2'(x) = \mathbf{L}_2\mathbf{f}_2'(x) - \overline{\mathbf{L}}_1\bar{\mathbf{f}}_1'(x) \tag{A.2}$$

by the standard analytic continuity argument

$$\mathbf{L}_1\mathbf{f}_1'(z) = \overline{\mathbf{L}}_2\bar{\mathbf{f}}_2'(z), \quad z \in 1. \tag{A.3}$$

Define the displacement jump across the interface as

$$\mathbf{d}(x) = \mathbf{u}(x, 0^+) - \mathbf{u}(x, 0^-) \tag{A.4}$$

with the aid of Eq. (A.3), a direct calculation is given by

$$\mathbf{t}(x) = \mathbf{L}_1\mathbf{f}_1'(x) + \mathbf{L}_2\mathbf{f}_2'(x), \tag{A.5}$$

$$\mathrm{i}\mathbf{d}'(x) = \mathbf{H}\mathbf{L}_1\mathbf{f}_1'(x) - \overline{\mathbf{H}}\mathbf{L}_2\mathbf{f}_2'(x). \tag{A.6}$$

According to the continuity of the displacement across the bonded interface as inferred from Eq. (A.6), implies that $\mathbf{L}_1\mathbf{f}_1'(x)$ and $\mathbf{L}_2\mathbf{f}_2'(x)$ can be analytically extended to the whole plane except on the crack line and satisfy

$$\mathbf{h}(z) = \mathbf{L}_1\mathbf{f}_1'(z) = \mathbf{H}^{-1}\overline{\mathbf{H}}\mathbf{L}_2\mathbf{f}_2'(z), \quad z \notin C, \tag{A.7}$$

where C is denoted as the crack line. Hence, one can focus on $\mathbf{h}(z)$, and once $\mathbf{h}(z)$ is obtained, the full-field solution could be given by Eq. (A.7). In terms of $\mathbf{h}(z)$, the traction (A.5) can be expressed as

$$\mathbf{t}(x) = \mathbf{h}^+(x) + \overline{\mathbf{H}}^{-1}\mathbf{H}\mathbf{h}^-(x), \quad z \in C \tag{A.8}$$

Appendix B

$$\Lambda_1(\xi, \eta, \beta) = \frac{1}{\eta - \xi}\sum_{k=1}^{2}\frac{[1 + \mu_k^2 + \mathrm{e}^{2\mathrm{i}\beta}(1 - \mu_k^2 - 2\mathrm{i}\mu_k)]B_k}{(1 - \mathrm{i}\mu_k)\mathrm{e}^{\mathrm{i}\beta} + (1 + \mathrm{i}\mu_k)\mathrm{e}^{-\mathrm{i}\beta}},$$

$$\Lambda_2(\xi,\eta,\beta)=\frac{1}{\eta-\xi}\sum_{k=1}^{2}\frac{[1+\overline{\mu_k}^2+\mathrm{e}^{2\mathrm{i}\beta}(1-\overline{\mu_k}^2-2\mathrm{i}\overline{\mu_k})]\overline{B_k}}{(1+\mathrm{i}\overline{\mu_k})\mathrm{e}^{-\mathrm{i}\beta}+(1-\mathrm{i}\overline{\mu_k})\mathrm{e}^{\mathrm{i}\beta}},$$

$$\Lambda_3(\xi,\eta,\beta,y_0)=-\frac{1}{2}\sum_{k=1}^{2}\sum_{j=1}^{4}\sum_{i=1}^{2}\frac{\overline{b_{kj}}m_{ji}[1+\overline{\mu_k}^2+\mathrm{e}^{2\mathrm{i}\beta}(1-\overline{\mu_k}^2-2\mathrm{i}\overline{\mu_k})]B_i}{(\eta-\xi)\cos\beta+(y_0+\eta\sin\beta)\overline{\mu_k}-(y_0+\xi\sin\beta)\mu_i},$$

$$\Lambda_4(\xi,\eta,\beta,y_0)=-\frac{1}{2}\sum_{k=1}^{2}\sum_{j=1}^{4}\sum_{i=1}^{2}\frac{b_{kj}\overline{m_{ji}}[1+\mu_k^2+\mathrm{e}^{2\mathrm{i}\beta}(1-\mu_k^2-2\mathrm{i}\mu_k)]\overline{B_i}}{(\eta-\xi)\cos\beta+(y_0+\eta\sin\beta)\mu_k-(y_0+\xi\sin\beta)\overline{\mu_i}},$$

$$\Lambda_5(\xi,\beta,x_0,y_0,\eta_1,\beta_1,x_{01},y_{01})=\frac{1}{2}\sum_{k=1}^{2}\frac{[1+\mu_k^2+\mathrm{e}^{2\mathrm{i}\beta_1}(1-\mu_k^2-2\mathrm{i}\mu_k)]B_k}{(x_{01}+\eta_1\cos\beta_1-x_0-\xi\cos\beta)+(y_{01}+\eta_1\sin\beta_1-y_0-\xi\sin\beta)\mu_k},$$

$$\Lambda_6(\xi,\beta,x_0,y_0,\eta_1,\beta_1,x_{01},y_{01})=\frac{1}{2}\sum_{k=1}^{2}\frac{[1+\overline{\mu_k}^2+\mathrm{e}^{2\mathrm{i}\beta_1}(1-\overline{\mu_k}^2-2\mathrm{i}\overline{\mu_k})]\overline{B_k}}{(x_{01}+\eta_1\cos\beta_1-x_0-\xi\cos\beta)+(y_{01}+\eta_1\sin\beta_1-y_0-\xi\sin\beta)\overline{\mu_k}},$$

$$\Lambda_7(\xi,\beta,x_0,y_0,\eta_1,\beta_1,x_{01},y_{01})=-\frac{1}{2}\sum_{k=1}^{2}\sum_{j=1}^{4}\sum_{i=1}^{2}\frac{\overline{b_{kj}}m_{ji}[1+\overline{\mu_k}^2+\mathrm{e}^{2\mathrm{i}\beta_1}(1-\overline{\mu_k}^2-2\mathrm{i}\overline{\mu_k})]B_i}{(x_{01}+\eta_1\cos\beta_1-x_0-\xi\cos\beta)+(y_{01}+\eta_1\sin\beta_1)\overline{\mu_k}-(y_0+\xi\sin\beta)\mu_k},$$

$$\Lambda_8(\xi,\beta,x_0,y_0,\eta_1,\beta_1,x_{01},y_{01})=-\frac{1}{2}\sum_{k=1}^{2}\sum_{j=1}^{4}\sum_{i=1}^{2}\frac{b_{kj}\overline{m_{ji}}[1+\mu_k^2+\mathrm{e}^{2\mathrm{i}\beta_1}(1-\mu_k^2-2\mathrm{i}\mu_k)]\overline{B_i}}{(x_{01}+\eta_1\cos\beta_1-x_0-\xi\cos\beta)+(y_{01}+\eta_1\sin\beta_1)\mu_k-(y_0+\xi\sin\beta)\overline{\mu_k}}. \tag{B.1}$$

Appendix C

$$\begin{aligned}J_\infty&=\int_{\Gamma_\infty}(w\,\mathrm{d}y-T_iu_{i,1}\,\mathrm{d}l),\\ J_t&=\int_{\Gamma_t}(w\,\mathrm{d}y-T_iu_{i,1}\,\mathrm{d}l),\\ \Delta J&=\oint_{\Gamma^*}(w\,\mathrm{d}y-T_iu_{i,1}\,\mathrm{d}l),\end{aligned} \tag{C.1}$$

$$\begin{aligned}J_1^*&=\oint_{\Gamma^*}(w^*\mathrm{d}y^*-T_i^*u_{i,1}^*\,\mathrm{d}l),\\ J_2^*&=\oint_{\Gamma^*}(-w^*\mathrm{d}x^*-T_i^*u_{i,2}^*\,\mathrm{d}l).\end{aligned} \tag{C.2}$$

References

Chen, Y.H., Hasebe, N., 1994a. Further investigation of comninou's EEF for an interface crack with completely closed face. Int. J. Engng. Sci. 32, 1037–1046.

Chen, Y.Z., Hasebe, N., 1994b. Eigenfunction expansion and higher order weight function of interface cracks. ASME J. Appl. Mech. 61, 843–849.
Chen, Y.H., 1996. On the contribution of discontinuities in a near-tip stress field to *J*-integral. Int. J. Engng. Sci. 34, 819–829.
Chen, Y.H., Ma, H., 1997. Explicit function expression of J_2 in anisotropic body. Sci. China 27, 310–317.
Gao, H., 1991. Weight function analysis of interface crack. ASME J. Appl. Mech. 58, 931–938.
Herrmann, A.G., Herrmann, G., 1981. A path-independent integral and the approximate analysis. ASME J. Appl. Mech. 48, 525–528.
Horii, H., Nemat-Nasser, S., 1985. Elastic field of interacting inhomogeneities. J. Mech. Phys. Solids 33, 731–745.
Hutchinson, J.W., 1987. Crack tip shielding by microcracking in brittle solids. Acta Metall. 35, 1605–1619.
Hutchinson, J.W., Mear, M.E., Rice, J.R., 1987. Crack paralleling an interface between dissimilar materials. ASME J. Appl. Mech. 54, 828–832.
Lekhnitskii, S.G., 1963. Theory of Elasticity of an Anisotropic Body. Holden-Day, San Francisco.
Lu, H., Lardner, T.J., 1992. Mechanics of subinterface crack in layered material. Int. J. Solids Struct. 29, 669–688.
Miller, G.R., 1989. Analysis of cracks near interfaces between dissimilar anisotropic materials. Int. J. Engng. Sci. 27 (6), 667–678.
Rice, J.R., 1968. A path-independent integral and the approximate analysis of strain concentration by notches and cracks. ASME J. Appl. Mech. 35, 379–386.
Rice, J.R., 1988. Elastic fracture mechanics concepts for interface cracks. ASME J. Appl. Mech. 55, 98–103.
Sih, G.C., Chen, E.P., 1981. Mechanics of Fracture, Cracks in Composite Materials. Martinus Nijhoff, The Netherlands.
Suo, Z., 1990. Singularities, interfaces and cracks in dissimilar anisotropic media. Proc. R. Soc. Lond. A 427, 331–358.
Ting, T.C.T., 1986. Explicit solution and invariance of the singularities at an interface crack in anisotropic composites. Int. J. Solids Struct. 22, 965–983.
Ting, T.C.T., 1990. Interface crack in anisotropic bimaterials. J. Mech. Phys. Solids 38, 505–513.
Wang, S.S., Choi, I., 1983a. The interface crack between dissimilar anisotropic composite materials. ASME J. Appl. Mech. 50, 169–178.
Wang, S.S., Choi, I., 1983b. The interface crack behavior in dissimilar anisotropic composites under mixed mode loading. ASME J. Appl. Mech. 50, 179–183.
Zhao, L.G., Chen, Y.H., 1997. On the contribution of subinterface microcrack near tip of an interface crack to the *J*-integral in bimaterial solids. Int. J. Engng. Sci. 35, 387–407.